Chemical Engineering Journal 286 (2016) 91–97

Contents lists available at ScienceDirect

Chemical Engineering Journal

journal homepage: www.elsevier.com/locate/cej

Photoelectrocatalytic hydrogen production by water splitting using $BiVO_4$ photoanodes

Olivier Monfort [a,1], Lucian-Cristian Pop [a], Stavroula Sfaelou [a], Tomas Plecenik [b], Tomas Roch [b], Vassilios Dracopoulos [c], Elias Stathatos [d], Gustav Plesch [e], Panagiotis Lianos [a,c,*]

[a] Department of Chemical Engineering, University of Patras, 26500 Patras, Greece
[b] Department of Experimental Physics, Faculty of Mathematics Physics and Informatics, Comenius University in Bratislava, Mlynská Dolina, 84248 Bratislava, Slovakia
[c] FORTH/ICE-HT, P.O. Box 1414, 26504 Patras, Greece
[d] Electrical Engineering Dept., Technological–Educational Institute of Western Greece, 26334 Patras, Greece
[e] Department of Inorganic Chemistry, Faculty of Natural Sciences, Comenius University in Bratislava, Mlynská Dolina, 84215 Bratislava, Slovakia

HIGHLIGHTS

- Bismuth vanadate photoanodes used for photoelectrochemical hydrogen production.
- Control of the mesostructure using surfactant templates.
- Structure optimization and extensive characterization.
- Use of a novel electrocatalyst for hydrogen generation.

GRAPHICAL ABSTRACT

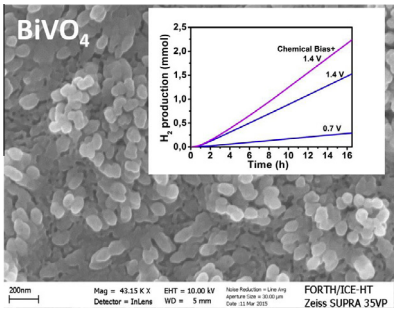

ARTICLE INFO

Article history:
Received 19 June 2015
Received in revised form 15 October 2015
Accepted 19 October 2015
Available online 23 October 2015

Keywords:
$BiVO_4$
Bismuth vanadate
Photoelectrochemical cells
Water splitting
Hydrogen production

ABSTRACT

Nanocrystalline bismuth vanadate was deposited by simple wet chemistry procedure on FTO electrodes in order to construct visible light responsive photoanodes, which were employed for photoelectrochemical hydrogen production by water splitting. The specific surface area of the films was controlled by the presence of a surfactant template (Triton X-100). It was, however, found that when the quantity of surfactant was relatively high, the stoichiometry of the photocatalyst as well as its activity was lost. The obtained materials were characterized by SEM, XRD, AFM, BET and UV–Vis spectroscopy. Optimized photoanodes were employed in photoelectrochemical cells for water splitting and hydrogen production under electric and chemical bias. Maximum hydrogen production rate was 0.15 mmol/h under electric bias of 1.4 V vs Ag/AgCl plus 0.37 V chemical bias.

1. Introduction

$BiVO_4$ is a medium band gap semiconductor, which has attracted attention as a visible light responsive photocatalyst for water splitting applications [1]. The most common and the only active polymorph of $BiVO_4$ takes a monoclinic scheelite-like crystalline structure with a band gap of 2.4 eV. Bismuth vanadate is a stable non-toxic yellow pigment and it is preferred from the similarly-colored CdS, which is toxic and easily photo-corroded. $BiVO_4$ conduction and valence band edges consist of vanadium 3d orbitals and a hybridization between oxygen 2p and bismuth 6s orbitals [1]. Its visible light absorption is related with bismuth 6s and vanadium 3d electron lone pairs, being located at relatively

* Corresponding author at: Department of Chemical Engineering, University of Patras, 26500 Patras, Greece.
E-mail address: lianos@upatras.gr (P. Lianos).
[1] Permanent address: Department of Inorganic Chemistry, Faculty of Natural Sciences, Comenius University in Bratislava, Mlynská Dolina, 84215 Bratislava, Slovakia.

http://dx.doi.org/10.1016/j.cej.2015.10.043
1385-8947/

positive potentials [1]. Monoclinic $BiVO_4$ was first developed by Kudo et al. [2] as water decomposition photocatalyst and has ever since been one of the most popular visible light responsive photocatalysts [1–9]. In 2003, Sayama et al. reported an IPCE value for photoelectrochemical water decomposition of 29% at 420 nm and by applying a bias of 1.9 V vs RHE [3]. More recently, Jie et al. attained a IPCE value of 73% at 420 nm by applying a bias of 1 V vs Ag/AgCl [4]. As a matter of fact, a bias is always necessary to obtain a substantial photocurrent by using $BiVO_4$ photoanodes, apparently, because electron–hole recombination is very important with this material. A broad list of obtained photocurrents under various applied bias and $BiVO_4$ structures is given in Ref. [8].

In the present work, we have studied $BiVO_4$ as photocatalyst for photoelectrochemical water splitting and hydrogen production. $BiVO_4$ has a conduction band edge located close to 0 V and a valence band edge close to 2.4 V vs NHE [6,7]. Therefore, it is well placed for effective water oxidation but necessitates a bias for water reduction. The maximum theoretical Solar-to-Hydrogen (STH) efficiency for monoclinic $BiVO_4$ of E_g = 2.4 eV is 9.1% [7,8], therefore, this photocatalyst is very promising, even though, the actual efficiencies obtained with pure $BiOV_4$ are much lower. STH efficiency for an unbiased photoelectrochemical cell, where the only input is incident radiation, is measured by the following formula [8]:

$$\eta_{STH} = \frac{J(\text{mA cm}^{-2}) \times 1.229(\text{V})}{I(\text{mW cm}^{-2})} \times 100\% \quad (1)$$

where J is the current density, I the intensity of the incident radiation and 1.229 V corresponds to the potential for water splitting [8]. For solar radiation AM 1.5 of 100 mW cm^{-2}, according to Eq. (1), it necessitates a photocurrent density of 7.4 mA cm^{-2} to reach the maximum theoretical STH efficiency of 9.1%. In practice, the obtained current is still smaller [10,11], especially for undoped $BiVO_4$, as it will become obvious also from the present results. Also in practice, the cell runs under bias, therefore the bias must be subtracted from 1.229 V and this makes efficiency smaller. These are some basic terms prescribing $BiVO_4$ behavior, however, what matters most with these materials is to adopt a simple protocol for their synthesis and deposition, which may allow their future utilization at the lowest possible cost. For this reason, we have adopted the most facile but optimized protocol of materials synthesis and application hoping to make the present work a handy reference on a material with great future ahead. $BiVO_4$ mesostructure is, in this work, to a certain degree controlled by surfactant templates while a novel material is introduced as reduction electrocatalyst for hydrogen production based on a combination of a stable carbon paste and a small quantity of dispersed Pt nanoparticles.

2. Experimental

2.1. Materials

Unless otherwise indicated, reagents were obtained from Aldrich and were used as received. Millipore water was used in all experiments. SnO_2:F transparent conductive electrodes (FTO, Resistance 8 Ω/square) were purchased from Pilkington, USA and carbon paste Elcocarb C/SP from Solaronix, Switzerland.

2.2. Photoanode electrodes made by deposition of $BiVO_4$ films on FTO

Nanoparticulate $BiVO_4$ films were deposited on FTO transparent electrodes by the following procedure, which is a modification of previously published procedures [6,12,13]. An FTO glass was cut in the appropriate dimensions and was carefully cleaned first with soap and then by sonication in acetone, ethanol, and water. Bismuth and vanadium precursor solutions were prepared by using bismuth nitrate pentahydrate and vanadium(III) acetylacetonate, respectively. Bismuth nitrate was dissolved in acetic acid and vanadium (III) acetylacetonate in acetylacetone. Solutions of 0.12 M were obtained for both precursors after sonication for 30 min. Then, 1 mL of each precursor solutions were mixed and sonicated until a deep green solution was obtained. In this mixture we added Triton X-100 as a structure control surfactant agent. The quantity of Triton ranged between 0.025 and 0.5 g/mL but the optimal concentration was 0.1 g/mL. For reasons of comparison, films were also deposited without any added surfactant. The as prepared sol was sonicated for 3 additional minutes. This sol was used to deposit a film by doctor blading, using Scotch tape as guide. The obtained film was annealed up to 500 °C for 10 min by using a heating ramp of 20 °C/min. This deposition-annealing procedure was repeated six times to make a film of about 350 nm thick, as measured by its SEM profile. The obtained film was ready for use and it was stored in the dark. The film area was 1.4 cm × 1.4 cm in the case of photoanodes used for IV measurements but larger electrodes were used for hydrogen production having an active film area of 3 cm × 4 cm.

2.3. Deposition of the electrocatalyst used for hydrogen production

The electrocatalyst was deposited on FTO by using the following procedure [14]: Commercial carbon paste named Elcocarb C/SP (Solaronix) was applied on FTO by doctor blading and was annealed at 450 °C. This paste forms a uniform and very stable film. Its quantity was 0.67 mg/cm^2. Elcocarb was mixed with Pt by deposition of a solution of Diamminedinitritoplatinum(II) in ethanol. The quantity of Pt contained in Elcocarb was 8 wt% (0.0536 mg/cm^2). The active area of the film was 3 cm × 4 cm.

2.4. Device (reactor) construction

We used two reactors, a small one made of Plexiglas and employed only for IV measurements and a large H-shaped reactor made of Pyrex glass and employed for hydrogen production. Current–voltage measurements were made by using the small reactor accommodating the small photoanode electrode with 1.4 cm × 1.4 cm active film area (see Section 2.2). In that case, a Pt foil (2.5 cm × 2.5 cm) was used as counter electrode. The reactor could also accommodate a Ag/AgCl reference electrode, when necessary. The quantity of the added electrolyte was 10 mL. In the case of hydrogen production we used a larger reactor, as already said, which could accommodate the large photoanode and cathode electrodes (3 cm × 4 cm active area, cf. Fig. 1 showing reactor design). The above Pt/Elcocarb/FTO electrode (Section 2.3) was used as cathode (counter) electrode. Hydrogen was collected on line by using Ar as carrier inert gas. Hydrogen was monitored either in the absence or under bias, using a few different electrolytes. The quantity of the electrolyte was 230 mL in each compartment of the cell. The two compartments were separated by a silica frit (ROBU, Germany, porosity SGQ 5, diameter 25 mm, thickness 2 mm). Optimal results were obtained with 0.5 M aqueous $NaHCO_3$. However, in some cases the reactor was operated under chemical bias where the electrolyte in the anode compartment was 0.5 M aqueous $NaHCO_3$ but in the cathode compartment it was 0.5 M H_2SO_4. In this large reactor, the reference electrode was placed in the anode compartment behind the photoanode electrode. Illumination of the photoanode was made in all cases by using a Xenon lamp set at about 100 mW cm^{-2}.

2.5. Measurements

Hydrogen was detected on line by using an SRI 8610C gas chromatograph. Calibration of the chromatograph signal was

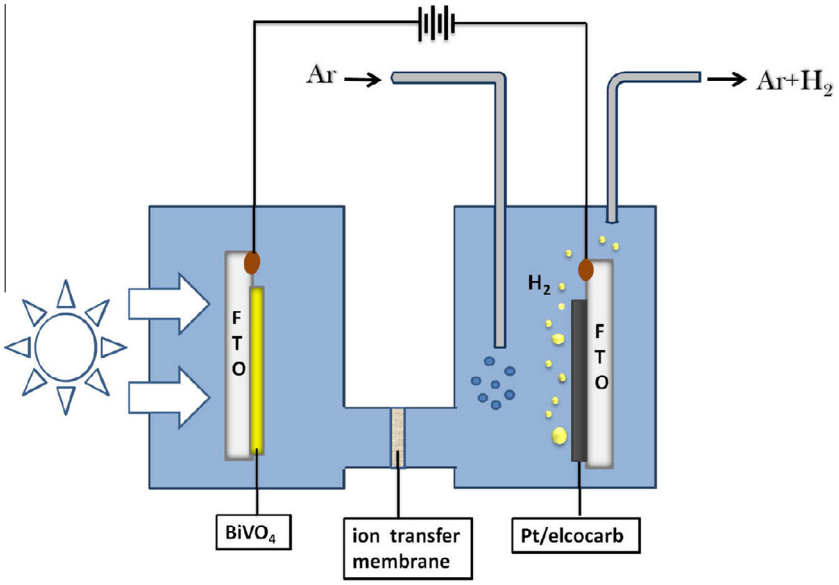

Fig. 1. Schematic representation of the H-shaped reactor employed for hydrogen production. A silica frit was used as ion transfer membrane. A reference electrode, when necessary, is placed in the photoanode compartment, which is exposed to the ambient).

accomplished by comparison with a standard of 0.25% H_2 in Ar. Application of electric bias and current–voltage curves were traced with the help of an Autolab potentiostat PGSTAT128N. UV–Vis diffuse reflectance spectra (DRS) were recorded with a Shimadzu model 2600 spectrophotometer and IPCE spectra with a Newport IQE 200 instrument. Nitrogen sorption/desorption curves were traced with a Micromeritics Tristar 3000 and surface area, porosity, and pore size distribution were derived by differentiating them according to the BET method. The morphology of the samples was observed with Field-Emission Scanning Electron Microscopy (FESEM, Zeiss SUPRA 35 VP) measurements. $BiVO_4$ films were characterized by X-ray diffraction (PANalytical XPert PRO MRD diffractometer), and atomic force microscopy (NT-MDT Solver P47 PRO). The XRD measurements have been performed using grazing incidence technique and PIXcel solid-state multichannel X-ray detector. The AFM surface analysis has been done in semicontact AFM mode using standard silicon AFM probes.

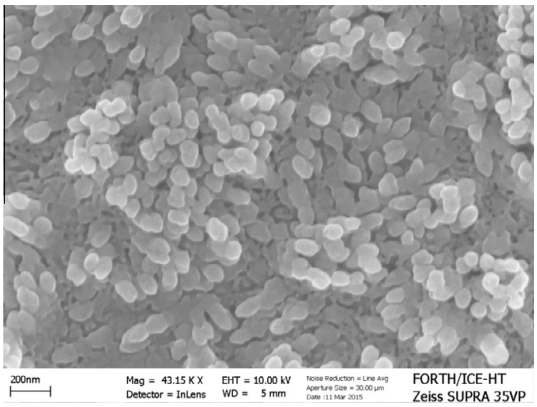

Fig. 2. FESEM image of a $BiVO_4$/FTO film made by using a precursor solution containing 0.1 g/mL Triton X-100. The scale bar is 200 nm.

3. Results and discussion

3.1. Characterization of the $BiVO_4$ films

$BiVO_4$ films were deposited on FTO glasses as described in Section 2.2. Most studied films were produced by using surfactant templates but some data were also obtained by using $BiVO_4$ photoanodes where the active component was deposited without added surfactant. The mesostructure of the film can be seen in the characteristic FESEM image of Fig. 2. The film consists of nanoparticles of a size roughly around 50 nm or smaller, which are coagulated forming larger mostly elongated nanoparticles. Corresponding TEM images (not shown) verified nanoparticle size. Fig. 3 shows XRD peaks for films made by using a few different quantities of surfactant template. The size of the nanoparticles, calculated by Scherrer's formula is listed in Table 1. Their size indeed ranged below 50 nm. The XRD diffractograms of Fig. 3 revealed the formation of monoclinic $BiVO_4$. However, at relatively high surfactant concentration, an unidentified species showed up with peaks appearing at angles mostly matching $Bi_4V_2O_{11}$ composition. The crystal sizes measured by Scherrer's formula marked a minimum for surfactant concentration equal to 0.1 g/mL. We believe that beyond this surfactant concentration no monoclinic $BiVO_4$ crystals are formed anymore.

BET porosimetry measurements were made by first depositing $BiVO_4$ film on FTO and then scratching the material off. Measurements were performed on the thus obtained powder. Compared to commonly used oxide semiconductor photocatalysts, like titania, $BiVO_4$ provides films with rather low specific surface S_{BET}. Indeed, as seen in Table 1, the latter ranged between 3.4 and 16.5 $m^2\ g^{-1}$. Films made for reasons of comparison by using titania Degussa P25 [14], gave S_{BET} equal to about 45 $m^2\ g^{-1}$. The presence of surfactant did affect porosity and specific surface, as can be seen in Table 1. Indeed, both specific surface and pore volume increased with increasing quantity of added Triton X 100 while pore diameter marked a minimum at surfactant content equal to 0.1 g/mL. Apparently, the latter is a limit surfactant content marking a change in material behavior in accordance with nanocrystal size extracted by XRD analysis. Samples made without any added surfactant were practically similar with those made with the lowest surfactant quantity. Corresponding AFM images, shown in Fig. 4, demonstrated a progressive decrease of cluster sizes with increasing surfactant concentration.

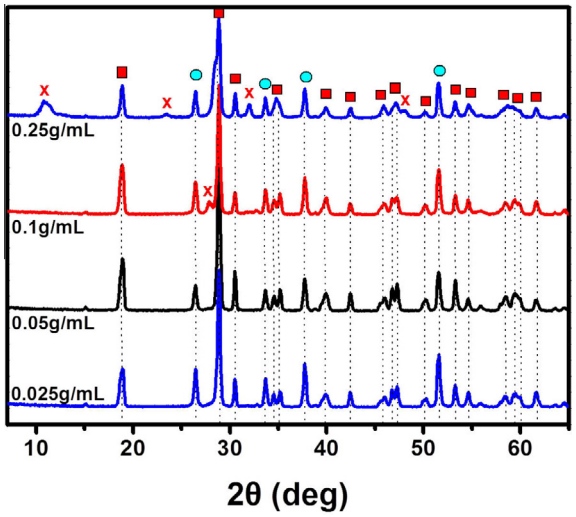

Fig. 3. XRD patterns of $BiVO_4$ films made by using precursor solutions containing various quantities of Triton X-100. Peaks marked with squares correspond to monoclinic $BiVO_4$, while circles correspond to the background FTO. Peaks marked with x correspond to a non-identified species showing up at high surfactant concentrations. (ICDD card Nos: 014-0688 and 042-0135).

Table 1
Characteristics of $BiVO_4$ films obtained by surfactant templating as a function of the quantity of the surfactant.

Quantity of Triton X-100 (g/mL)	XRD-extracted particle size (nm)	S_{BET} (m^2/g)	Pore diameter (nm)	Pore width (nm)	Pore volume (cm^3/g)
0	–	3.4	18.6	9.3	0.008
0.025	34.5	3.5	18.5	9.4	0.008
0.05	34.9	9.3	6.8	7.2	0.016
0.10	22.8	12.7	6.0	6.4	0.020
0.25	46.3	13.5	11.8	14.8	0.050
0.50	49.0	16.5	10.5	13.4	0.055

One main reason for studying $BiVO_4$ is its substantial capacity to absorb visible light. The presently made $BiVO_4$/FTO films had a yellow color (cf. Fig. S1 in Supplementary Material) and absorbed light up to 505 nm with a tail extending to 600 nm. This is seen in Fig. 5. The tail was inactive in the present case as seen by the action spectra shown in the same figure (more related discussion appears below).

3.2. Current–Voltage characteristics of the $BiVO_4$ photoanodes

The current density–voltage characteristics of a $BiVO_4$ photoanode were plotted for three different aqueous electrolytes without any additives and they are presented in Fig. 6. In all cases, the photoanode gave a substantial photocurrent, which was markedly higher and better-defined in the case of $NaHCO_3$. NaOH was not a "good" electrolyte for $BiVO_4$ photoanodes, since the originally yellow film lost its color after operation and became black, indicating a chemical reaction with this electrolyte. The photoanode preserved its color and its other characteristics in Na_2SO_4 and $NaHCO_3$ electrolytes. The onset for anodic photocurrent was observed around 0.5 V vs RHE. These current–voltage characteristics are necessary knowledge in order to define the conditions for hydrogen production using $BiVO_4$ photoanodes. Hydrogen in the present case is produced by reduction of water or hydrogen ions through water splitting processes. Reduction takes place at the counter electrode by electrons arriving though the external circuit. Therefore, it is expected that the quantity of hydrogen should be roughly proportional to the external current. Since the anodic onset is at 0.5 V vs RHE, it is expected that at least 0.5 V anodic (forward) bias is necessary in order to produce hydrogen. This prerequisite was verified by photoelectrochemical hydrogen production measurements, as will be analyzed below.

One question to be faced concerning the efficiency of the $BiVO_4$ photoanodes is related with the active surface area of the $BiVO_4$ films. In principle, active surface should depend on the quantity of the added structure-control agent, i.e. Triton X-100 surfactant. Fig. 7 shows the current density–voltage curves recorded with three $BiVO_4$ photoanodes made by using three different surfactant concentrations. Substantial photocurrent was produced with the photoanodes made with at least 0.05 g/mL of this structure-control agent. Maximum photocurrent was obtained with 0.1 g/mL while for larger quantities of surfactant the obtained film was of bad quality and the current smaller. This result matches the data of Table 1. Apparently, there is a limit to the quantity of surfactant in order to preserve a structural integrity of the films. In addition, there is a strong indication that the stoichiometry of $BiVO_4$ may not be preserved at high surfactant concentration. As already discussed and seen in Fig. 3, a non-identified species has been formed at higher surfactant concentrations. XRD peaks for this species better fit $Bi_4V_2O_{11}$. This species is apparently photoelectrocatalytically inactive and works against efficiency. It was then decided to use 0.1 g/mL as optimal surfactant content. The films obtained under these optimized conditions were employed for water splitting and hydrogen production. $NaHCO_3$ was employed as the optimal electrolyte for this purpose.

3.3. Action spectra of the $BiVO_4$/FTO photoanodes

As it has been already said, hydrogen production necessitates electron flow through the external circuit of the cell. In order to demonstrate that the $BiVO_4$/FTO photoanodes are active in the visible part of the spectrum we have studied their action spectra and the results are presented by the corresponding IPCE% values shown in Fig. 5. There is first a perfect matching with absorption spectrum, which corresponds to the band gap of monoclinic $BiVO_4$ [1]. Obviously monoclinic $BiVO_4$ is the active species as expected and observed in other works. Fig. 5 shows that the efficiency of the photoanode dramatically depends on the applied bias. The presently highest recorded IPCE% values were obtained by applying a bias of 1.4 V vs Ag/AgCl (2.08 V vs RHE), which is lower but comparable with the value recently obtained in Ref. [4]. The present results confirm the observation that, in the case of $BiVO_4$ photoanodes, a substantial current (and hydrogen production) may be expected only by applying a relatively strong forward bias.

3.4. Hydrogen production by water splitting

Fig. 8 gives hydrogen production rates by photoelectrochemical water splitting using the above described and optimized $BiVO_4$/FTO photoanodes. The reactor was the one illustrated in Fig. 1. The counter electrode was an FTO glass bearing Pt/Elcocarb paste as electrocatalyst (see Section 2.3). Hydrogen was indeed produced at substantial rates, which depended on the applied bias. As expected, for bias below 0.5 V vs RHE no hydrogen at all was detected. The rate of hydrogen production could be further enhanced by applying a chemical bias. In that case, the electrolyte in the cathode compartment was 0.5 M H_2SO_4. This provides an additional bias of 0.37 V = 0.059(8.2–2.0) V, where 8.2 and 2.0 are the pH values for 0.5 M $NaHCO_3$ and 0.5 M H_2SO_4, respectively. This difference was only slightly modified during the 16 h of hydrogen production. At the end of the process the pH at the anode became 8.0 while that of the cathode increased to 2.2. The corresponding cumulative hydrogen production is shown in Fig. 8B.

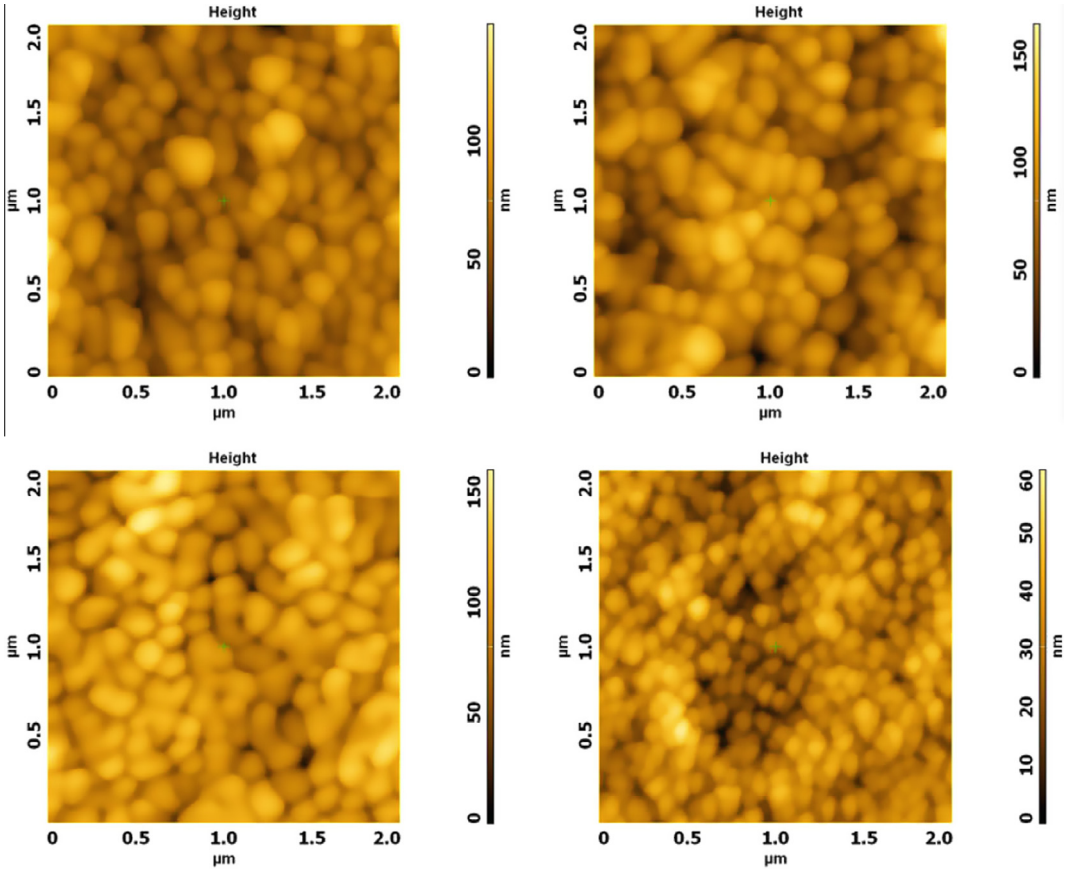

Fig. 4. AFM images of films made with precursor solutions containing various quantities of Triton X 100. From upper left to lower right: 0.025, 0.05, 0.1 and 0.25 g/mL.

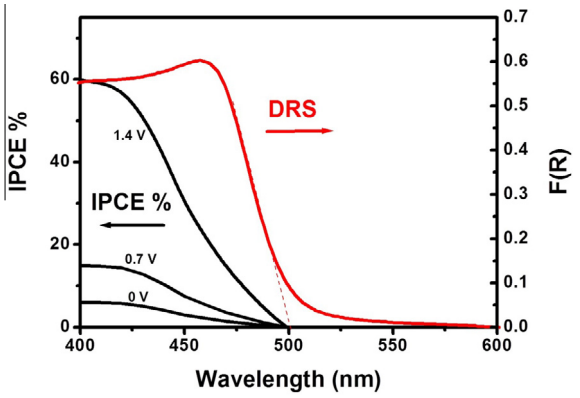

Fig. 5. Diffuse reflectance absorption (DRS) spectrum of a $BiVO_4$/FTO photoanode and corresponding IPCE% spectra. The latter were obtained by employing a cell containing 0.5 M $NaHCO_3$ as electrolyte and by applying a forward bias of 0, 0.7 and 1.4 V vs Ag/AgCl (0.68, 1.38 and 2.08 V vs RHE). The absorption spectrum has a threshold at 505 nm (2.45 eV, which, according to the literature, corresponds to the band gap of monoclinic $BiVO_4$).

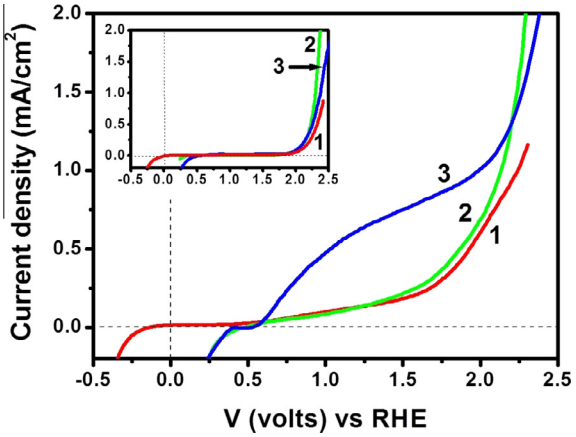

Fig. 6. Current Density–Voltage curves traced by using $BiVO_4$ photoanodes, platinum foil as counter and Ag/AgCl as reference electrode, in the presence of three different aqueous electrolytes: (1) Na_2SO_4; (2) NaOH; and (3) $NaHCO_3$. The electrolyte concentration was 0.5 M in all cases without any additives. The insert gives the corresponding dark currents. All curves were plotted vs RHE by shifting recorded curves according to the relation $\Delta V(\text{Volts}) = 0.2 + 0.059x(\text{pH})$, where 0.2 corresponds to the potential of the Ag/AgCl electrode vs SHE. The corresponding pH values were: 7.4 (Na_2SO_4); 8.2($NaHCO_3$); and 13.0 (NaOH).

The current flowing through the external circuit of the cell was monitored throughout the whole process. We observed an initial increase of around 30% and then it remained practically constant. The maximum hydrogen production rate was approximately 0.15 mmol/h and is considered satisfactory for non-doped $BiVO_4$ (cf. Refs. [4,12,15]). In this respect, the assets of the present work is the use of a two compartment cell separating reductive hydrogen from oxidative oxygen production and the employment of the mixture of carbon nanoparticles with a small quantity of Pt that makes an effective electrocatalyst, as it has been recently shown in other works [14,16,17].

The presence of an optimized quantity of surfactant template during film deposition was reflected also on the rate of hydrogen

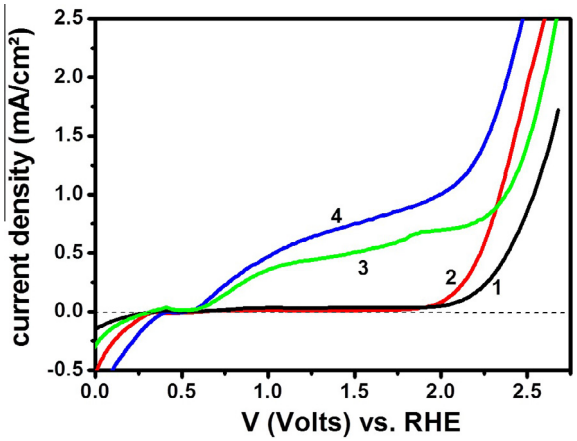

Fig. 7. Current Density–Voltage curves traced by using $BiVO_4$ photoanodes, platinum foil as counter and Ag/AgCl as reference electrode, in the presence of 0.5 M aqueous $NaHCO_3$, as a function of the Triton X-100 content in the precursor solution used for film deposition (g/mL): (1) dark current; (2) 0.025; (3) 0.05; and (4) 0.1.

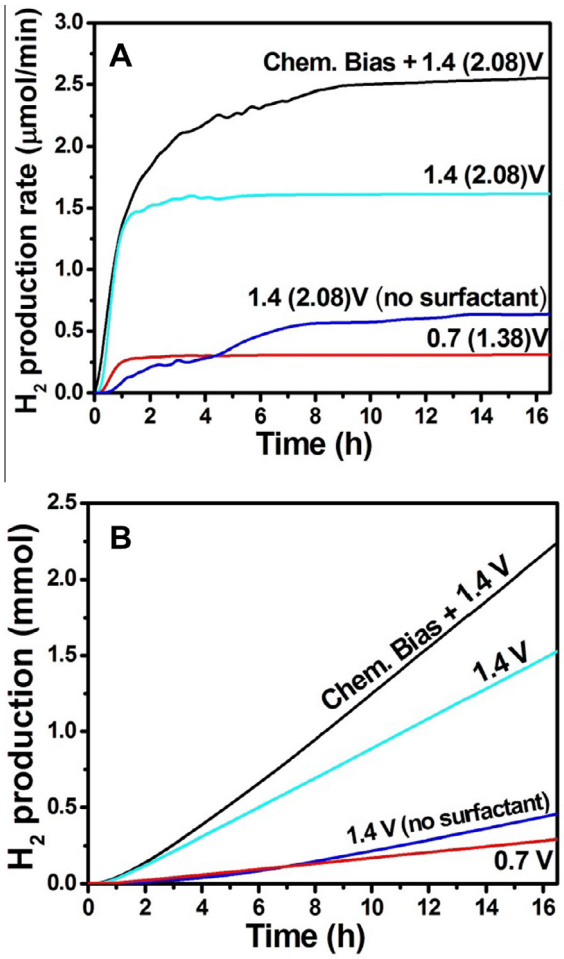

Fig. 8. Hydrogen production rate (A) and cumulative hydrogen production (B) using the optimal $BiVO_4$ photoanode and a photoanode made without surfactant templates. The label numbers correspond to voltages vs Ag/AgCl and in parentheses vs RHE.

production. As seen in Fig. 8, when the $BiVO_4$ film was deposited without templates, its hydrogen production ability was very poor compared with the templated film under the same conditions.

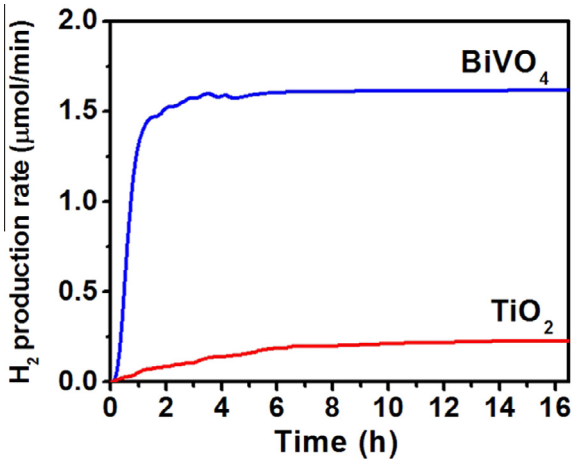

Fig. 9. Comparison of hydrogen production rates between TiO_2 and $BiVO_4$ photoanodes monitored under similar conditions.

A final point to make in this subsection is the data of Fig. 9. In this last figure, hydrogen production rate obtained with the optimal $BiVO_4$ photoanode is compared with the corresponding data obtained with a nanoparticulate TiO_2 photoanode made by using Degussa P25. Titania films were deposited on FTO electrodes by following the same route as in Refs. [14,16]. Care was taken to deposit approximately the same quantity of titania photocatalyst as $BiVO_4$. When hydrogen production was monitored under the same conditions, a small quantity of hydrogen was produced in the case of titania, obviously thanks to the absorption of light in the UV part of the exciting radiation. The merits of using a visible light absorbing photocatalyst are obvious by the data of Fig. 9.

4. Conclusions

Nanocrystalline bismuth vanadate makes a successful visible-light responsive photocatalyst for hydrogen production by photoelectrochemical water splitting. The merits of visible light response are obvious by direct comparison with a UV absorbing photocatalyst like titania. Synthesis and deposition of nanoparticulate $BiVO_4$ photoanodes can be achieved under simple chemical procedures and at ambient conditions. The presence of surfactant template helps increasing specific surface area of the photocatalyst, however, at too high surfactant concentrations, $BiVO_4$ stoichiometry is lost together with its photocatalytic activity.

Acknowledgements

This project is implemented under the "ARISTEIA" Action of the "OPERATIONAL PROGRAMME EDUCATION AND LIFELONG LEARNING" and is co-funded by the European Social Fund (ESF) and National Resources (Project No. 2275).

Olivier Monfort wishes to acknowledge a grant provided by the Scientific Grant Agency of the Slovak Republic (Project VEGA 1/0276/15) and the National Scholarship Program of the Slovak Republic managed by SAIA n.o. and funded by the Ministry of Education, Sport, Science and Research of the Slovak Republic which allowed his stay in the University of Patras.

Appendix A. Supplementary material

Supplementary data associated with this article can be found, in the online version, at http://dx.doi.org/10.1016/j.cej.2015.10.043.

References

[1] J. Gan, X. Lu, Y. Tong, Towards highly efficient photoanodes: boosting sunlight-driven semiconductor nanomaterials for water oxidation, Nanoscale 6 (2014) 7142–7164.

[2] A. Kudo, K. Ueda, H. Kato, I. Mikami, Photocatalytic O_2 evolution under visible light irradiation on $BiVO_4$ in aqueous $AgNO_3$ solution, Cat. Lett. 53 (1998) 229–230.

[3] K. Sayama, A. Nomura, Z. Zou, R. Abe, Y. Abe, H. Arakawa, Photoelectrochemical decomposition of water on nanocrystalline $BiVO_4$ film electrodes under visible light, Chem. Commun. 2908–2909 (2003).

[4] Q. Jia, K. Iwashina, A. Kudo, Facile fabrication of an efficient $BiVO_4$ thin film electrode for water splitting under visible light irradiation, PNAS 109 (2012) 11564–11569.

[5] Z. Huang, I. Pan, J. Zou, X. Zhang, L. Wang, Nanostructured bismuth vanadate-based materials for solar-energy-driven water oxidation: a review on recent progress, Nanoscale 6 (2014) 14044–14063.

[6] P. Chatchai, Y. Murakami, S. Kishioka, A.Y. Nosaka, Y. Nosaka, Efficient photocatalytic activity of water oxidation over $WO_3/BiVO_4$ composite under visible light irradiation, Electrochim. Acta 54 (2009) 1147–1152.

[7] S. Moniz, S.A. Shevlin, D. Martin, Z. Guo, J. Tang, Visible-light driven heterojunction photocatalysts for water splitting – a critical review, Energy Environ. Sci. (2015), http://dx.doi.org/10.1039/C4EE03271C.

[8] Z. Li, W. Luo, M. Zhang, J. Feng, Z. Zou, Photoelectrochemical cells for solar hydrogen production: current state of promising photoelectrodes, methods to improve their properties, and outlook, Energy Environ. Sci. 6 (2013) 347–370.

[9] S. Hernandez, G. Barbero, G. Saracco, A.-L. Alexe-Ionescu, Considerations on oxygen bubbles formation and evolution on $BiVO_4$ porous anodes used in water splitting photoelectrochemical cells, J. Phys. Chem. C 119 (18) (2015) 9916–9925.

[10] L. Zhang, C.-Y. Lin, V.K. Valev, E. Reisner, U. Steiner, J.J. Baumberg, Plasmonic enhancement in $BiVO_4$ photonic crystals for efficient water splitting, Small 10 (2014) 3970–3978.

[11] L. Han, F.F. Abdi, R. van de Krol, R. Liu, Z. Huang, H.-J. Lewerenz, B. Dam, M. Zeman, A.H.M. Smets, Efficient water-splitting device based on bismuth vanadate photoanode and thin-film silicon solar cells, ChemSusChem. 7 (2014) 2832–2838.

[12] K. Sayama, A. Nomura, T. Arai, T. Sugita, R. Abe, M. Yanagida, T. Oi, Y. Iwasaki, Y. Abe, H. Sugihara, Photoelectrochemical decomposition of water into H_2 and O_2 on porous $BiVO_4$ thin-film electrodes under visible light and significant effect of Ag ion treatment, J. Phys. Chem. B 110 (2006) 11352–11360.

[13] X. Zhang, S. Chen, X. Quan, H. Zhao, Preparation and characterization of $BiVO_4$ film electrode and investigation of its photoelectrocatalytic (PEC) ability under visible light, Sep. Purif. Technol. 64 (2009) 309–313.

[14] L.-C. Pop, V. Dracopoulos, P. Lianos, Photoelectrocatalytic hydrogen production using nanoparticulate titania and a novel Pt/Carbon electrocatalyst: the concept of the "Photoelectrocatalytic Leaf", Appl. Surf. Sci. 333 (2015) 147–151.

[15] R. Saito, Y. Miseki, K. Sayama, Photoanode characteristics of multi-layer composite $BiVO_4$ thin film in a concentrated carbonate electrolyte solution for water splitting, J. Photochem. Photobio. A: Chem. 258 (2013) 51–60.

[16] L.-C. Pop, I. Tantis, P. Lianos, Photoelectrocatalytic hydrogen production using nitrogen containing water soluble wastes, Int. J. Hydrogen Energy 40 (26) (2015) 8304–8310.

[17] R. Michal, S. Sfaelou, P. Lianos, Photocatalysis for renewable energy production using photofuelcells, Molecules 19 (2014) 19732–19750.